

# Global Model of Differential Rotation in the Sun

Steven A. Balbus<sup>1,2,4</sup>, Henrik Latter<sup>1,3</sup>, Nigel Weiss<sup>3</sup>

## ABSTRACT

The isorotation contours of the solar convective zone (SCZ) show three distinct morphologies, corresponding to two boundary layers (inner and outer), and the bulk of the interior. Previous work has shown that the thermal wind equation together with informal arguments on the nature of convection in a rotating fluid could be used to deduce the shape of the isorotation surfaces in the bulk of the SCZ with great fidelity, and that the tachocline contours could also be described by relatively simple phenomenology. In this paper, we show that the form of these surfaces can be understood more broadly as a mathematical consequence of the thermal wind equation and a narrow convective shell. The analysis does not yield the angular velocity function directly, an additional surface boundary condition is required. But much can already be deduced without constructing the entire rotation profile. The mathematics may be combined with dynamical arguments put forth in previous works to the mutual benefit of each. An important element of our approach is to regard the constant angular velocity surfaces as an independent coordinate variable for what is termed the “residual entropy,” a quantity that plays a key role in the equation of thermal wind balance. The difference between the dynamics of the bulk of the SCZ and the tachocline is due to a different functional form of the residual entropy in each region. We develop a unified theory for the rotational behavior of both the SCZ and the tachocline, using the solutions for the characteristics of the thermal wind equation. These characteristics are identical to the isorotation contours in the bulk of the SCZ, but the two deviate in the tachocline. The outer layer may be treated, at least descriptively, by similar mathematical techniques, but this region probably does not obey thermal wind balance.

---

<sup>1</sup>Laboratoire de Radioastronomie, École Normale Supérieure, 24 rue Lhomond, 75231 Paris CEDEX 05, France [steven.balbus@lra.ens.fr](mailto:steven.balbus@lra.ens.fr)

<sup>2</sup>Institut universitaire de France, Maison des Universités, 103 blvd. Saint-Michel, 75005 Paris, France

<sup>3</sup>DAMTP, Wilberforce Road, Cambridge CB3 0HA, UK

<sup>4</sup>Princeton University Observatory, Peyton Hall, Princeton University, Princeton NJ 08540

## 1. Introduction

Helioseismology has revealed a global pattern of differential rotation in the solar convective zone (SCZ) comprising three distinct, readily apparent, regions. In the bulk of the SCZ (region 1), the isorotation contours appear mainly as quasi-radial spokes in meridional planes (corresponding in three dimensions to cones). The contours change relatively little and only very gradually near the poles and equator, but in the boundary between the SCZ and the uniformly rotating radiative interior (the “tachocline”), the isorotation contours are abruptly wrenched into quasi-spherical shells (region 2). Finally, in the outermost few percent of the Sun’s exterior layers, the SCZ isorotation spokes gradually acquire lengthening tangential tails stretching from the parent spoke toward the equator (region 3). The challenge for the theorist is to account for this global organization as economically as possible, a task that motivates the current paper.

Despite the intrinsic dynamical complexity of a rotating, convecting fluid there are some indications that the solar rotation profile may obey rather simple mathematical laws. In particular, much of the convective zone may be governed by a reduced form of the vorticity equation, known as the thermal wind equation, or TWE (Thompson et al. 2003). The TWE involves a balance between inertial angular velocity gradients and baroclinic driving, the latter arising from angular entropy gradients that may be present.

The TWE is not, by itself, sufficient to solve for the rotation profile, since it is a single equation containing two unknowns, the angular velocity  $\Omega$  and entropy  $S$ . It has been suggested, however, that  $S$  and  $\Omega$  may be *a priori* functionally related, and that this relationship could be exploited to solve the TWE. For example, Balbus (2009) pointed out that a certain class of magnetized baroclinic modes were marginally stable if constant  $S$  and  $\Omega$  surfaces coincided. With  $S$  a function of  $\Omega$  only, the TWE can be formally, but quite usefully, solved. The solution does not yield the entire spatial structure of  $\Omega$ , rather it yields a parameterized form for the surfaces on which  $\Omega$  is a constant (see equation [3], below). The fit to the data is strikingly good.

In a subsequent analysis, Balbus et al. (2009; hereafter BBLW) argued that magnetic fields were not essential to establishing the  $S - \Omega$  functional relationship. Under conditions expected in the SCZ, the effect of differential rotation on thermally convecting cells will be to distort surfaces of constant entropy into surfaces of constant angular velocity  $\Omega$ . More precisely, one expects the surfaces of constant *residual* entropy—the portion of the entropy in excess of the destabilizing radial entropy profile needed to drive convection—to tend to coincide with surfaces of constant angular velocity. In the TWE, a functional relation between residual entropy  $S'$  and  $\Omega$  works just as well as an  $S - \Omega$  functional relationship, since it is only the angular derivatives of  $S$  that enter into the equation: the difference

between  $S$  and  $S'$  is a function only of radius  $r$ . But the distinction between residual and total entropy is of course otherwise important. In numerical simulations of the SCZ that most closely resemble the Sun, for example, surfaces of constant  $S$  are nearly spherical shells, whereas surfaces of constant  $S'$  indeed correspond much more closely to those of constant angular velocity (Miesch, Brun, & Toomre 2006).

The mathematical implementation of the constraint of shared surfaces of constant residual entropy and rotation may be written

$$S(r, \theta) = f(\Omega^2) + S_r(r) \quad (1)$$

where  $S(r, \theta)$  is the entropy,  $r$  and  $\theta$  are the standard spherical radius and colatitude angle,  $\Omega$  is the angular velocity,  $f$  is an arbitrary function of  $\Omega^2$ , and  $S_r$  is the spherical entropy profile needed to drive and maintain convection. Equation (1) is then equivalent to the statement that the residual entropy  $S' \equiv S - S_r$  is constant on a surface of constant  $\Omega^2$ .

On a strictly mathematical level, however,  $S_r$  need not be a particular entropy profile—in equation (1), it evidently could be any function of  $r$  at all. Within the theory of BBLW,  $S_r$  itself is never directly used in constructing the rotation profile. Instead, it is  $f(\Omega^2)$  that is important. The arbitrariness of  $S_r$  endows equation (1) with a much greater generality than is obvious at first glance, a point that we will develop in §2 of this work.

If the ansatz (1) is used in the governing dynamical equation (the azimuthal component of the vorticity equation), a self-contained quasi-linear partial differential equation emerges for  $\Omega^2$  whose characteristics are precisely the isorotation curves of region 1. These contours take the very simple mathematical form

$$r^2 \sin^2 \theta = A - B/r \quad (2)$$

where  $A$  and  $B$  are constant along a given curve<sup>1</sup>; this basic structure is in excellent agreement with the helioseismology data (BBLW). If the isorotation curve passes through some colatitude angle  $\theta_0$  at some radius  $r = r_0$ , then the explicit equation for the isorotation curves is

$$\sin^2 \theta = \left(\frac{r_0}{r}\right)^2 \left[ \sin^2 \theta_0 - \beta \left(\frac{r_0}{r} - 1\right) \right]. \quad (3)$$

The dimensionless parameter  $\beta$  is a number of order unity, which might be different for different contours.

It may be possible to develop this formalism to explain the structure of the isorotation contours even beyond the bulk interior of the SCZ. Recently, Balbus & Latter (2010, hereafter BL) argued that a tachocline structure resembling that of the Sun emerges from the

---

<sup>1</sup>More generally,  $r^2 \sin^2 \theta = A + B\Phi(r)$ , where  $\Phi$  is the gravitational potential (Balbus & Weiss 2010).

assumption of a simple  $P_2$  spherical harmonic vorticity source that is present inside of some transition radius  $r_T$ , and is otherwise  $r$ -independent. More precisely, if  $\mathcal{D}/\mathcal{D}r$  represents the radial derivative taken along a  $\theta(r)$  characteristic given by equation (3), and if  $C$  is a constant, then the equation

$$\frac{\mathcal{D}\Omega^2}{\mathcal{D}r} = CP_2(\cos\theta) \quad (4)$$

reproduces the SCZ isorotation contours for  $C = 0$ , and is able to closely describe the tachocline isorotation contours for  $C < 0$ . The angular velocity remains continuous at the transition radius  $r = r_T$ ; its derivative along the characteristic is discontinuous. In the bulk of the SCZ, the TWE characteristics and the isorotation contours are indistinguishable. Within the tachocline, they are very different curves.

This development is quite suggestive, hinting that an understanding of the Sun’s internal differential rotation may not require a detailed dynamical knowledge of convective turbulence. Instead, the powerful constraint of thermal wind balance may be used to determine the angular velocity profile  $\Omega(r, \theta)$  that is created by turbulent transport. At the same time, important questions arise which motivate the current work. In this paper, there is perhaps some progress toward elucidating some answers. But much remains to be done, particularly for the subsurface outer layers.

*Why is the match between mathematical solution and observations so good in the bulk of the SCZ?* There seems to be a curious mismatch between the ability of the mathematical  $r^2 \sin^2 \theta = A - B/r$  curves to reproduce the helioseismology data so strikingly, and the more qualitative physical arguments that motivate the precise form of the thermal wind equation that is used. The theory seems to work too well. We would not expect, for example, constant residual entropy and constant angular velocity surfaces to match *exactly*. We would expect there to be a *tendency* to follow one another, and the most solar-like numerical simulations do show such a tendency (Miesch et al. 2006). But assuming an exact match leads to precise agreement between calculation and helioseismology observations. Is there something more going on here?

*Does thermal wind balance necessarily break down in the tachocline?* BL did, in fact, interpret their equation this way, but is this essential? Is it possible to retain thermal wind balance with a different functional relation between angular velocity and residual entropy that keeps the goodness of fit intact?

*What is the physical explanation for the angular structure of the tachocline isorotation contours?* Both the helioseismic morphology and the rotational dynamics seem to be completely dominated by quadrupolar-like forcing. Why? For that matter, how accurately do we know that the angular behavior of the vorticity stress? Is it precisely quadrupolar?

*What is happening in the Sun’s outer layer?* Do turbulent stresses become important (Miesch & Hindman 2011)? Can we guess the form of a simple  $\theta$ -dependent forcing as was done for the tachocline? The surface distortion of the isorotation contours does not display  $P_2$  symmetry, it is strictly monotonic from pole to equator. The simplest possibility is  $\sin^2 \theta$  forcing. How well does this work, and what is its physical origin?

An outline of the paper is as follows. In §2, we review the results of earlier work (BBLW, BL) in which it was shown that thermal wind balance and informal arguments were used to construct precise mathematical solutions for the isorotation contours in the bulk of the SCZ through the tachocline. We then show that the all-important relationship between the residual entropy and  $\Omega^2$  must be true in a well-defined and physically interesting asymptotic limit, independently of other dynamical complications. These “complications,” however, are likely to broaden the range of validity of the asymptotic limit. In §3, we construct a global, thermal wind model for the Sun’s differential rotation profile, and show that it compares favorably with the helioseismology data. The outer layers are treated on an ad hoc basis, with a deeper investigation of the issues presented in an Appendix. The change in the form of the isorotation contours apparent upon entering the tachocline does not indicate a breakdown of global thermal wind balance, but instead a local functional dependence of the residual entropy on both angular velocity and colatitude angle  $\theta$ . In §4, we present a physical discussion of our results, explore its limitations, and suggest directions for future research.

## 2. Thermal wind balance in the solar convection zone

### 2.1. Pure rotation model: governing equation

Throughout this paper, we will work with both spherical  $(r, \theta, \phi)$  and cylindrical  $(R, \phi, z)$  coordinates. As noted in the Introduction,  $r$  and  $\theta$  are respectively the spherical radius and colatitude angle. The quantity  $\phi$  is the azimuthal angle, while  $R$  and  $z$  are the cylindrical radius and vertical Cartesian coordinate respectively.

The governing dynamical equation of our analysis is the  $\phi$  component of the vorticity equation. For steady flows this is

$$(\rho \mathbf{v} \cdot \nabla) \left( \frac{\omega_\phi}{r \sin \theta} \right) - (\boldsymbol{\omega} \cdot \nabla) \Omega = \frac{1}{(r \sin \theta) \rho^2} (\nabla \rho \times \nabla P) \cdot \mathbf{e}_\phi \quad (5)$$

or, since by mass conservation  $\nabla \cdot (\rho \mathbf{v}) = 0$ ,

$$\nabla \cdot \left[ \frac{\mathbf{v} \omega_\phi}{R} - \boldsymbol{\omega} \Omega \right] = \frac{1}{R \rho} (\nabla \ln \rho \times \nabla P) \cdot \mathbf{e}_\phi \quad (6)$$

where  $\mathbf{v}$  is the velocity,  $\omega$  the vorticity,  $P$  the pressure, and  $\rho$  is the density. Equation (6) implicitly defines a vorticity flux within the divergence operator on its left side. The vector  $\mathbf{e}_\phi$  is of unit norm, in the azimuthal direction.

The left side of equation (5) contains two terms, the first corresponding to advection by the poloidal velocity components of the vortensity (divided by cylindrical radius), the second to vorticity distortion by differential rotation. For a purely azimuthal velocity field, only the second (vorticity-distorting) term is present. This leads to what is commonly referred to as the *thermal wind equation* (Thompson et al. 2003):

$$-\cos\theta\left(\frac{\partial\Omega^2}{\partial r}\right)_\theta + \frac{\sin\theta}{r}\left(\frac{\partial\Omega^2}{\partial\theta}\right)_r \equiv -\left(\frac{\partial\Omega^2}{\partial z}\right)_R = \frac{1}{(r\sin\theta)\rho}(\nabla\ln\rho\times\nabla P)\cdot\mathbf{e}_\phi. \quad (7)$$

An important simplification of equation (7) is effected by replacing, with impunity,  $\ln\rho$  by  $-(1/\gamma)\ln P\rho^{-\gamma}$ , where  $\gamma$  is the adiabatic index. Then, in terms of the entropy variable  $\sigma = \ln P\rho^{-\gamma}$  and gravitational field  $g = -(1/\rho)(\partial P/\partial r)$ , we have:

$$\left(\frac{\partial\Omega^2}{\partial r}\right)_\theta - \frac{\tan\theta}{r}\left(\frac{\partial\Omega^2}{\partial\theta}\right)_r = \frac{g}{\gamma r^2 \sin\theta \cos\theta}\left(\frac{\partial\sigma}{\partial\theta}\right)_r \quad (8)$$

On the right side, we have dropped the term proportional to  $(\partial\sigma/\partial r)(\partial P/\partial\theta)$  in favor of  $(\partial\sigma/\partial\theta)(\partial P/\partial r)$ . This is justified because, while the radial gradient of  $\sigma$  may well exceed its  $\theta$  gradient in the SCZ (region 1), because of entropy mixing by convection it does so by a factor far smaller than the pressure radial gradient exceeds *its*  $\theta$  gradient. We will adopt equation (8) as our governing equation, though it must break down, of course, inside the radiative zone (cf. §3).

## 2.2. Establishing a functional relation between $\sigma$ and $\Omega^2$

As discussed in the Introduction and in BBLW, the entropy variable  $\sigma$  appears in equation (8) only in the form of its  $\theta$  gradient. This means that any function differing from  $\sigma$  by another function depending only upon  $r$  would serve just as well as  $\sigma$  itself. There is, in other words, a gauge invariance in the problem<sup>2</sup>.

This observation motivated BBLW to introduce the residual entropy  $\sigma'$ , defined by

$$\sigma'(r, \theta) = \sigma(r, \theta) - \sigma_r(r) \quad (9)$$

---

<sup>2</sup> A similar issue formally afflicts the angular velocity, which is insensitive to an additive function of  $R$ . This “geostrophic degeneracy” is lifted by fitting our  $\Omega$  solution to an explicit set of isrotation surfaces provided by observations.

where  $\sigma_r$  is the minimal adverse radial entropy profile needed to both drive and maintain ongoing convection. In this manner, we choose our gauge. The idea is that mixing of entropy would eliminate *residual* entropy gradients within a convective cell, but the resulting nearly constant value of  $\sigma'$  within one convective cell need not be the same constant in another cell. BBLW went on to argue that the presence of shear would favor the tendency for long-lived coherent convective structures to lie also within constant  $\Omega$  surfaces. Under these conditions, constant  $\sigma'$  and constant  $\Omega$  surfaces would tend to coincide.

The mathematical implementation of this is a powerful analytic constraint. If  $\sigma' = f(\Omega^2)$ , where  $f$  is a function to be determined, then

$$\sigma(r, \theta) = f(\Omega^2) + \sigma_r(r) \quad (10)$$

(cf. equation [1]). In this view, the combination of convection and rotation in the SCZ constrains the two-dimensional entropy to be an *additive* function  $\Omega^2$  and  $r$ .

Let us take a somewhat more formal viewpoint for the moment. On purely mathematical grounds, for this development to be valid, all that is required is that the constraint embodied by equation (10) be satisfied for whatever reason. If it is, the ensuing thermal wind partial differential equation becomes

$$\left( \frac{\partial \Omega^2}{\partial r} \right)_\theta - \left[ \frac{\tan \theta}{r} + \frac{gf'(\Omega^2)}{\gamma r^2 \rho \sin \theta \cos \theta} \right] \left( \frac{\partial \Omega^2}{\partial \theta} \right)_r \equiv \frac{\mathcal{D}\Omega^2}{\mathcal{D}r} = 0, \quad (11)$$

where  $f'(\Omega^2)$  is  $df/d\Omega^2$ , and we have made use of the  $\mathcal{D}$  notation of equation (4). The solution to equation (11) is that  $\Omega$  is constant along the contours given explicitly by equation (3). It is remarkable that no knowledge of  $f$  is necessary to extract the basic functional form of the contours:  $R^2$  is just a linear function of  $1/r$ . Since these simple contours lie essentially on top of the helioseismology data (BBLW), the mathematical formalism at the very least constrains any deeper physical theory for the origin of  $\Omega(r, \theta)$ . Equation (10) and thermal wind balance are empirically true. The ultimate underlying physical cause remains to be settled, however: the physical argument laid out in BBLW may or may not be the correct one.

### 2.3. Another approach to the $\sigma' - \Omega^2$ relationship

In addition to a likely dynamical linkage between  $\sigma'$  and  $\Omega$ , there is another simple feature of our problem that supports equation (10) : the SCZ is rather thin.

Imagine a Sun-like star with a slender outer convective zone. In the case of the SCZ itself, the central radius is about  $r_c = 0.87r_\odot$  and our analysis extends  $\pm 0.1r_\odot$ , so the

relative spread in the radial domain  $\Delta r/r_c$  is some 11.5%. The residual entropy  $\sigma'$  is a two-dimensional function of  $r$  and  $\theta$ , but it could equally well be locally regarded, by the implicit function theorem, as a function of  $r$  and  $\Omega^2$  (the sign of  $\Omega$  should not matter)<sup>3</sup>. We shall assume this is valid throughout the SCZ. Our motivation for choosing these two quantities as independent variables, as opposed to, e.g. angular momentum and  $r$ , is clear: we wish to turn the thermal wind equation into a simple mathematical constraint for the surfaces of constant  $\Omega$ . Had  $\Omega^2$  not been one of our dependent variables, the task of extracting the form of the constant isorotation contours from the thermal wind equation would be much more difficult. Much the same technique is familiar in thermodynamics, where the choice of functions for independent variables is somewhat arbitrary, but often dictated by what quantity is being held constant during the transformation of interest.

If the dispersion in  $\Omega^2$  and  $r$  in the SCZ is such that  $\sigma'(\Omega^2, r)$  never leaves the bilinear regime, then equation (10) will be directly satisfied, with gauge invariance allowing us to use either  $\sigma$  or  $\sigma'$ . But an expansion in  $\Omega^2$  is not essential. If we expand  $\sigma'(\Omega^2, r)$  in a Taylor series about  $r = r_c$ , there obtains

$$\sigma'(\Omega^2, r) \simeq \sigma'(\Omega^2, r_c) + \left(1 - \frac{r_c}{r}\right) \left(\frac{\partial \sigma'}{\partial \ln r}\right)_\Omega + \dots \quad (12)$$

The second term, which we shall regard as a small, is reduced relative to the first by an explicit factor of  $1 - r/r_c \simeq 0.1$ . But, as we argued in the Introduction, if in the dynamical regime of the SCZ there is already some tendency for constant  $\sigma'$  and  $\Omega$  surfaces to coincide, which is another way of saying that *any partial derivative of  $\sigma'$  taken at constant  $\Omega$  will be small*. The point is that “small” is by no means infinitesimal: the first-order correction to retaining the leading term in equation (12) is quadratic, not linear in small quantities. Two 10% effects would combine to yield a 1% effect. It is the mutually reinforcement of the tendency of  $\sigma'$  and  $\Omega$  surfaces to blend (even if it is not more than a trend), plus the narrow shell approximation  $|r - r_c| \ll r_c$ , that renders the  $\sigma'(r, \theta) = \sigma'(\Omega^2)$  ansatz more robust than might at first sight seem apparent. The narrowness of the shell means that residual entropy variations are more beholden to changes in  $\Omega$  than to the spread in  $r$ , and the process of convection reinforces this trend by constraining the radial residual entropy gradients (at constant  $\Omega$ ). The Sun happens to be in a felicitous theoretical regime from this point of view: it has both an order unity convective Rossby number (Miesch & Toomre 2009) and a relatively narrow convective layer.

---

<sup>3</sup>There are of course some technical restrictions that accompany this remark. The variable  $\Omega^2$  should be well-behaved, free of internal extrema or saddle points over the domain of interest; surfaces of constant  $\Omega$  should not be spherical. These are not concerns for our present application.



Is it at all useful to consider the dependence  $\sigma'(\Omega^2, \theta)$ ? This seems counterproductive in the SCZ, where  $\Omega$  already has a dominant  $\theta$  dependence, and where we have just advanced arguments to the effect that  $\sigma'$  should be considered a function of  $\Omega^2$  alone. But we can also turn this argument around. In the tachocline,  $\Omega$  is clearly dominated by its  $r$  dependence. Therefore, from a global viewpoint, adopting a  $\sigma'(\Omega^2, \theta)$  dependence would allow both the tachocline and the SCZ to be treated on the same footing, without necessarily abandoning thermal wind balance. In this formalism,  $\sigma'$  goes from a two-dimensional function in the tachocline  $(\Omega^2, \theta)$  to a simpler one-dimensional function in the SCZ  $(\Omega^2)$ . Such a dynamical structure would not be unknown in the study of rotating fluids: a classical two-dimensional Ekman boundary layer joining onto a one-dimensional interior Taylor column exhibits the same feature. In §3, this idea will be more fully developed.

## 2.4. Intuitively understanding the convection zone

### 2.4.1. Mathematical description

The current approach has helped us to understand the answer to the first question posed in the Introduction: why do informal arguments work so well when our mathematical solutions are compared with observations? It is enlightening to examine the mathematical form of our simple SCZ solution with a view toward the helioseismology data.

Let us start with the explicit solution (3) for an isorotation contour in the form

$$\sin^2 \theta = \frac{\sin^2 \theta_0 + \beta}{y^2} - \frac{\beta}{y^3} \quad (13)$$

where  $y = r/r_0$ . Then, expanding about some fiducial radius  $y_c$ ,

$$\sin^2 \theta = \left( \frac{\sin^2 \theta_0 + \beta}{y_c^2} - \frac{\beta}{y_c^3} \right) + (y - y_c) \left( \frac{3\beta}{y_c^4} - \frac{2\sin^2 \theta_0 + 2\beta}{y_c^3} \right) + \dots \quad (14)$$

which implies the existence of a constant  $\theta$  contour (a radial spoke) if

$$y_c = \frac{1.5\beta}{\sin^2 \theta_0 + \beta} \quad (15)$$

lies within the convection zone. The data show that in fact it does so for  $\theta_0 \simeq 30^\circ$ . For other angles not too near the poles or equator, the deviation from this class of contour is evidently not large. But neither is the alignment perfect: at larger  $\theta_0$  the spoke is canted more parallel to the  $z$  axis, while at smaller  $\theta_0$  the cant is more orthogonal to the vertical direction. All this can be seen both in the helioseismology data, and the leading order term of a Taylor expansion of our simple solution.

### 2.4.2. Dynamics

What is special about  $\Omega \simeq \Omega(\theta)$  that much of the convection zone is to first order well-described by this class of contour? It is by no means a direct consequence of our  $\sigma' = f(\Omega^2)$  ansatz, yet it is the most striking feature of the SCZ, and must involve the dynamics of heat convection and rotation. We defer an extended discussion of this important point to a subsequent paper (Schaan & Balbus 2011), but the basic picture is easily grasped. The coupled dynamics of entropy and angular velocity gradients are indeed at the heart of matter. The most efficient route for heat transport is spherical convection, radial motions being the most direct path to the surface. However, an inevitable secondary consequence of turbulent convection in an initially uniformly rotating system is the production of differential rotation, a sort of dynamical pollutant in this case. The presence of differential rotation introduces its own inertial force, pushing fluid parcels away from spherically radial motions toward *cylindrically* radial motions. For a displacement  $\boldsymbol{\xi}$ , this acceleration is of the form  $-\boldsymbol{\xi} \cdot \nabla \Omega^2$ . (Note that this is *not* the Coriolis force.) If spherical radial displacements dominate, this oblateness-inducing force is formally eliminated when  $\Omega = \Omega(\theta)$ . Radially convecting elements could then not help but move in constant  $\Omega$  surfaces. This closes the circle of theoretical self-consistency: the gross pattern of differential rotation in the Sun looks the way it does because in the presence of unavoidable build-up of differential rotation,  $\Omega \simeq \Omega(\theta)$  would produce a pattern that would not interfere with the most efficient form of heat transport. The top priority of the convective zone would remain uncompromised. Moreover, we have in the previous section noted that the description of the  $\Omega$  curves is *not* precisely  $\Omega(\theta)$ ; the curves are canted slightly poleward everywhere but at the highest latitudes. This slight poleward cant emerges, in fact, from the linear theory of convective displacements (Schaan & Balbus 2011) as well, and  $\boldsymbol{\xi} \cdot \nabla \Omega^2$  remains small.

## 3. Global solutions of the isorotation contours

### 3.1. Entering the tachocline

As one crosses from the SCZ into the tachocline, the isorotation contours change their character abruptly. It is possible that this is due to the increased importance of additional dynamics beyond pure rotational motion, and the thermal wind equation breaks down. On the other hand, there is little reason to assume that the precise  $\sigma' - \Omega^2$  relation in the SCZ should hold here; the  $r$  component of  $\nabla \Omega$  becomes vastly more important in the tachocline. Let us assume that thermal wind balance continues to hold in the tachocline. We will make use of the ansatz  $\sigma' = \sigma'(\Omega^2, \theta)$ , which is particularly apt, since  $\Omega$  now carries a

strong  $r$ -dependence. This pronounced dependence on radius is of course a consequence of the boundary condition enforcing uniform rotation at the radiative zone interface. Once this zone is breached, the radial entropy gradient starts to rise, and the approximation of neglecting the term proportional to  $\partial s/\partial r$  in the baroclinic contribution to the thermal wind equation eventually breaks down. But by this point,  $\Omega$  will be so close to uniform rotation that the shift of the isorotation contours is unlikely to be important.

We turn now to an investigation of thermal wind balance in the tachocline.

### 3.2. The ansatz $\sigma' = \sigma'(\Omega^2, \theta)$

The thermal wind equation acquires a very different mathematical structure if  $\sigma'$  is taken to be a function of  $\Omega^2$  and  $\theta$ , as opposed to  $\Omega^2$  and  $r$ . We will assume that this functional dependence is well-defined locally in  $r$  for the tachocline region. The, the equation formally becomes

$$\frac{\partial \Omega^2}{\partial r} - \left[ \frac{\tan \theta}{r} + \frac{g}{\gamma r^2 \sin \theta \cos \theta} \left( \frac{\partial \sigma'}{\partial \Omega^2} \right)_\theta \right] \frac{\partial \Omega^2}{\partial \theta} = \frac{g}{\gamma r^2 \sin \theta \cos \theta} \left( \frac{\partial \sigma'}{\partial \theta} \right)_{\Omega^2}. \quad (16)$$

This should be contrasted with the case  $\sigma' = \sigma'(\Omega^2, r)$ , for which the equation takes the form

$$\frac{\partial \Omega^2}{\partial r} - \left[ \frac{\tan \theta}{r} + \frac{g}{\gamma r^2 \sin \theta \cos \theta} \left( \frac{\partial \sigma'}{\partial \Omega^2} \right)_r \right] \frac{\partial \Omega^2}{\partial \theta} = 0. \quad (17)$$

What is striking here is that equation (16) has precisely the same mathematical form invoked by BL to account for the rotation pattern in the tachocline. (The computed rotation pattern fit the data well.) But this earlier study viewed the right side of the equation as arising from *external* vorticity stresses. Here, we see that this same equation could equally well arise without the need to appeal to external dynamics, emerging instead within the context of thermal wind balance.

Notice the important distinction between  $\partial \sigma'/\partial \Omega^2$  at constant  $\theta$  versus constant  $r$ . At constant  $\theta$ , the derivative is perfectly well behaved in the tachocline. At constant  $r$ , the derivative is ill-behaved: a significant change in  $\sigma'$  can be accompanied by virtually no change in  $\Omega$ . For this reason, equation (16) is to be preferred.

Comparison of equations (16) and (17) reveals another simple but important fact. If  $\sigma'$  is a function of  $\Omega^2$  alone in the SCZ (and it certainly appears to be so), equation (16) is valid globally. The partial  $\theta$  derivative on the right vanishes in the SCZ, and comes alive within the tachocline. At the very least, this is a useful organizational framework for understanding solar rotation. The truly daunting problem of mastering the underlying dynamics of the

tachocline can be decoupled from the strictly mathematical problem of finding self-consistent solutions to equation (16). For the latter, we may appeal directly to the observations, and to very general and simple dynamical constraints. While not directly addressing the underlying physical structure of the tachocline, this approach is not without interest: a compelling fit would be strong evidence for the assumption of thermal wind balance.

### 3.3. Tachocline solution

In BL, the characteristics of the SCZ continued into the tachocline, and the entire inhomogeneous term on the right side of the governing equation was assumed to be proportional to a function of  $\theta$  only, the spherical harmonic  $P_2(\cos \theta)$ .

In the current theoretical formalism, we have created somewhat tighter mathematical constraints for ourselves. The SCZ characteristics can now extend into the tachocline (which BL found produced good agreement with the data) only if  $(\partial\sigma'/\partial\Omega^2)_\theta$  is a function of  $\Omega^2$  alone. This means that  $(\partial\sigma'/\partial\theta)_{\Omega^2}$  can be a function only of  $\theta$ . This in turn means that the right side inhomogeneous term of equation (16) has a steep  $g/r^2 \sim 1/r^4$  radial dependence. This radial dependence was *not* present in BL, since the entire transition zone (from  $0.77r_\odot$  to  $0.65r_\odot$ ) was viewed as a local boundary layer. How does the additional radial dependence, a new feature of the current model, affect the shape of the tachocline isorotation contours?

In the tachocline, equation (16) may be written

$$\frac{\mathcal{D}\Omega^2}{\mathcal{D}r} = \frac{g}{\gamma r^2 \sin \theta \cos \theta} \left( \frac{\partial\sigma'}{\partial\theta} \right)_{\Omega^2}. \quad (18)$$

The  $\theta$  dependence of the right side of the equation may be inferred from helioseismology data as being approximately proportional to  $-P_2(\cos \theta)$ , or  $\sin^2 \theta - 2/3$ . We will consider a slightly more general form,  $\sin^2 \theta - \epsilon$ , allowing  $\epsilon$  to be determined by the best fit. (Note that the  $\theta$  dependence of  $\sigma'$  itself must then involve a superposition of  $P_4(\cos \theta)$  and  $P_2(\cos \theta)$ , as found in the simulations of Miesch et al. [2006].) Consider the equation

$$\frac{\mathcal{D}\Omega^2}{\mathcal{D}r} = \frac{C}{r^4}(\sin^2 \theta - \epsilon). \quad (19)$$

The formal solution to equation (19) is that  $\Omega^2(r)$  is given along a characteristic curve by

$$\Omega^2(r) = \Omega^2(r_1) + \int_{r_1}^r \frac{C}{r^4} [\sin^2 \theta(r) - \epsilon] dr \quad (20)$$

with

$$\sin^2 \theta(r) = \left( \frac{r_0}{r} \right)^2 \left[ \sin^2 \theta_0 - \beta \left( \frac{r_0}{r} - 1 \right) \right]. \quad (21)$$

The coordinates  $r_0$  and  $\theta_0$  represent the starting and defining point of the characteristic (the effective surface), and  $r_1$  is a fiducial radius marking here the starting point of the tachocline. In general, we will use equation (20) with  $r < r_1$ , reversing the integration limits and changing the sign. The  $\beta$  parameter in general will depend upon  $\theta_0$ , though it is simplest to take  $\beta$  to be a global constant, and we will often do so. The radius  $r_0$  will always lie outside of the tachocline on the constant- $\Omega$  portion of the characteristic. We use the notation  $r_1 = r_T$  for start of the SCZ-tachocline boundary, and we may take  $\Omega^2(r_1) = \Omega_0^2(\sin^2 \theta_0)$ . Then, along a characteristic (21), the variation of angular velocity is given by

$$\Omega^2(r) = \Omega_0^2(\sin^2 \theta_0) + \epsilon C F_3 - C r_0^2 (\beta + \sin^2 \theta_0) F_5 + C \beta r_0^3 F_6 \quad (22)$$

where

$$F_j = F_j(r, r_T) = \int_r^{r_T} \frac{du}{u^{j-1}} = \frac{1}{j} \left( \frac{1}{r^j} - \frac{1}{r_T^j} \right) \quad (23)$$

To apply this with a minimum of mathematical overhead to an interesting case, consider a linear form for  $\Omega_0^2(\sin^2 \theta_0)$ ,

$$\Omega_0^2(\sin^2 \theta_0) = \Omega_1^2 + \Omega_2^2 \sin^2 \theta_0, \quad (24)$$

with  $\Omega_1^2$  and  $\Omega_2^2$  constants. This may be regarded as a simplified model of the Sun's surface.

For this particular form of  $\Omega_0^2(\sin^2 \theta_0)$ , the solution for  $\Omega^2(r, \theta)$  is found by eliminating  $\sin^2 \theta_0$  between equations (21) and (22). The equation for the isorotational contours is then found to be

$$\sin^2 \theta = \left( \frac{r_0}{r} \right)^2 \left[ \frac{\Delta - \epsilon c_1 r_0^3 F_3 + \beta c_1 r_0^5 F_5 - \beta c_1 r_0^6 F_6}{1 - c_1 r_0^5 F_5} + \beta \left( 1 - \frac{r_0}{r} \right) \right] \quad (25)$$

where we define the dimensionless constants  $\Delta$  and  $c_1$  by

$$\Delta = \frac{\Omega^2 - \Omega_1^2}{\Omega_2^2}, \quad c_1 = \frac{C}{r_0^3 \Omega_2^2} \quad (26)$$

Note that the contour-labeling collection of constants comprising the quantity  $\Delta$  is numerically the same as  $\sin^2 \theta_0$ . By choosing  $c_1$  and  $\epsilon$  appropriately, equation (25) represents a global solution for both the bulk of the SCZ and the tachocline.

### 3.4. The outer layer

In the outermost layer of the Sun,  $r > 0.96 r_\odot$ , the convection is likely to be vigorous, with velocities comparable to the sound speed. In this zone, there is no reason to expect

that a simple thermal wind balance prevails in the vorticity equation, and good reason to suspect that turbulent forcing is involved (Miesch & Hindman 2011). For deriving the form of the isorotation contours however, it is useful to have a simple phenomenological description of this region. An inspection of the helioseismology data indicates a  $\sin^2 \theta$  rotational morphology in the subsurface layers. We have accordingly found that setting

$$\frac{\mathcal{D}\Omega^2}{\mathcal{D}r} = \frac{C_o \sin^2 \theta}{r_\odot - r} \quad (27)$$

works extremely well as a governing equation for the outer layer isorotation contours. The right side of this equation is a departure from thermal wind balance, and may be the outcome of some combination of convectively-induced Reynolds stresses, meridional circulation, and magnetic braking. Here, as earlier,  $\mathcal{D}/\mathcal{D}r$  is the radial derivative along the SCZ contour, and  $C_o$  is a universal constant. In the formalism of Miesch & Hindman (2011) the baroclinic term is dropped, whereas here it is incorporated in the  $\mathcal{D}/\mathcal{D}r$  operator. The right side of equation (27) would then correspond to the  $\mathcal{G}$  term of Miesch & Hindman, divided by  $R \cos \theta$ . Whatever the origin of the right side forcing of (27), this equation may be solved for the constant  $\beta$  case by characteristic techniques entirely analogous to those used for the tachocline solution (25). In fact, the equations are simpler, since  $r$  may be set equal to  $r_\odot$  everywhere, save the expression  $r - r_\odot$ .

An investigation of the form of equation (27) based on retaining poloidal circulation terms in the vorticity conservation equation (5) is presented in the Appendix. We find that the  $\sin^2 \theta$  dependence can be readily reproduced in such a picture, but the singular  $1/(r_\odot - r)$  behavior seems to require additional dynamics. It is possible that the increasingly steep radial entropy gradient plays a role via the as yet neglected baroclinic term proportional to the product of  $\partial P/\partial \theta$  and  $\partial \sigma/\partial r$ .

### 3.5. Results

#### 3.5.1. Constant and varying $\beta$

The analytic solutions that extend our characteristic techniques into the tachocline and SCZ boundaries are rigorous, we reemphasize, only if the  $\beta$  parameter is a universal constant. Otherwise there is a nontrivial coupling between the characteristic equations for  $d\theta/dr$  and  $d\Omega^2/dr$  in the boundary layers. (But not, it must be stressed, in the bulk of the SCZ, which may be handled rigorously in the case of a varying  $\beta$ .) We will develop accurate numerical models for this case in a later study, but for the present we will begin with constant  $\beta$  models. These work well enough (remarkably so given their simplicity) to foster

confidence in our fundamental approach. We will then take our expressions for the constant  $\beta$  solutions, and in effect abuse them by using the same expressions with a varying  $\beta$  chosen to match the contours in the bulk of the SCZ. Ignoring the differential equation couplings this would introduce with the tachocline is justified if such couplings were small, here a marginal assumption. But the effect of this simple expediency on the boundary layer isorotation curves produces an extremely striking match to the data (cf. Figure [5]). This strongly motivates pursuing a more rigorous numerical solution of the governing partial differential equation, a project we defer to a later publication.

Figures (1-3) show the constant  $\beta$  isorotation contours (equation [25]) for  $\beta = 0.55$ , 0.84, and 1.1 respectively. The first value is chosen to match high latitude structure, the second to match the diverging tachocline contours at  $\theta \simeq 60^\circ$ , and the final  $\beta$  value to match the equatorial contour structure. Overall, the global constant  $\beta$  models clearly resemble the helioseismology data of figure 4. In particular, the large  $\beta$  contours near the bifurcation point of the tachocline display a “plateau” followed by a precipitate, cliff-like structure that is evident in the data.

In figure (5) we have overlayed the data with an analytic solution. To effect this, we have used equation (25) but with  $\beta$  a function of  $\sin \theta_0$ :

$$\beta = 2.5 \sin^2 \theta_0 - 2.113 \sin \theta_0 + .8205. \quad (28)$$

The overlay shows an excellent, detailed, global match.

### 3.5.2. What is $\epsilon$ ?

In figures (1-3),  $\epsilon$  has been set to 0.75. This parameter sets the location at which the isorotation contours bifurcate in the tachocline. What sets its value?

BL set  $\epsilon$  equal to  $2/3$  on the basis that this fit the data rather well, and because  $\sin^2 \theta - 2/3$  was proportional to the spherical harmonic  $P_2[\cos(\theta)]$ , a natural leading order structural modification to spherical symmetry. But a closer investigation shows that there is a better data fit. In figures (5) and (6) we show overlay plots with  $\epsilon = 2/3$  and  $4/5$  respectively. While these fits are reasonable, they are clearly inferior to  $\epsilon = 3/4$ . Is there something special about this value of  $\epsilon$ ?

One possible explanation is dynamical. For example, what is the torque exerted by our solution on the inner, uniformly rotating radiative zone? We assume that the couple is proportional to  $R\partial\Omega/\partial r$ , the  $r\phi$  component of a viscous stress tensor. We denote

$$\epsilon_n = \frac{n+1}{n+2} \quad (29)$$

so that  $\epsilon_1$ ,  $\epsilon_2$ , and  $\epsilon_3$  correspond to our three choices. Then the following elementary integral identity is satisfied:

$$\int_0^\pi \sin^n \theta (\sin^2 \theta - \epsilon_n) d\theta = 0. \quad (30)$$

The case  $n = 3$  is relevant to the calculation of the torque exerted by the tachocline on the inner uniformly rotating core since this torque is directly proportional to the integral on the left side of the equation. (One factor of  $\sin \theta$  arises from the  $r\phi$  stress tensor component, another from the lever arm  $r \sin \theta$ , and the third from the spherical area element.) In other words, when  $\epsilon = \epsilon_3 = 0.8$ , the torque exerted by the tachocline on the interior vanishes. Since the couple to the core must act on time scales no shorter than evolutionary, we might therefore expect  $\epsilon = 0.8$  to yield the best fit.

The best fit, however, is clearly  $\epsilon = \epsilon_2 = 0.75$ . This is close enough to 0.8 that there may be something correct about our argument, but far enough off the mark that there is surely a piece of the puzzle missing. Moreover, it really is the case that  $\epsilon = 3/4$  is the best fit in our models, not just among the three values we display here. While there is no compelling reason to believe that the value of  $\epsilon$  may be accurately deduced from the idealized assumption of a vanishing viscous torque, it is puzzling that an equally simple, but quite distinguishable, integral constraint seems to fit the data so well. It is as though we had mistakenly included an additional factor of  $\sin \theta$  inside our viscous torque integral.

For the present, the explanation for why  $\epsilon = \epsilon_2 = 0.75$  and not  $\epsilon_3 = 0.8$ , corresponding to a true vanishing stress at colatitude  $\theta = 60^\circ$  rather than  $3.4^\circ$  further south, remains elusive.

## 4. Summary

In this paper, we have investigated global models of the angular rotation profile of the solar convective zone (SCZ) using the toroidal component of the vorticity equation and under the assumption of a dominant thermal wind balance. The model is global in that it seeks to unite both the tachocline and the bulk of the SCZ within the thermal wind formalism. The subsurface outer layers have also been treated at a quantitative, but more descriptive, level. In effect, we have modeled the subsurface outer layers by an ad hoc source term to the thermal wind equation.

The general nature of the isorotation surfaces in the joint SCZ-tachocline structure seems to be a mathematical consequence of a few simple principles, each noncontroversial by itself: i) thermal wind balance, as noted above; ii) a narrow SCZ which may be treated locally in  $r$ ; iii) a tendency for surfaces of constant angular velocity and residual entropy (see



below) to blend; iv) an inner boundary condition of uniform rotation at the tachocline base; v) vigorous radial transport in the bulk of the SCZ; vi) a small couple between the tachocline and the core. When modeled by an idealized viscous prescription and the simplest possible deviation from spherical symmetry, assumption vi gives close, but not perfect, agreement with helioseismology data.

As in earlier studies (e.g. BBLW, BL), we have introduced and exploited the concept of residual entropy, in essence the true entropy minus a suitable average over angles. The residual entropy is, in fact, defined only up to an additive function of  $r$ . Numerical simulations are particularly well suited to this concept: a Schwarzschild-unstable, user-determined entropy profile  $S(r)$  is imposed to drive the requisite convective turbulence, and what one may call the “response” entropy  $\tilde{S}(r, \theta)$  is then the quantity that is calculated (e.g. Miesch & Toomre 2009 and references therein). While  $\tilde{S}$  may formally differ from the residual entropy  $S'$  by compensating the radial background  $S(r)$ , in practice it is not difficult to extract a suitable  $S'$  from the numerical simulations.

The heart of our approach is to regard the two-dimensional residual entropy as a function of  $\Omega^2$  and  $\theta$  in the tachocline, but a function of  $\Omega^2$  and  $r$  in the bulk of the SCZ. In §2.3 we have argued that the  $r$  dependence of  $\sigma'$  within the SCZ is ultimately unimportant. In fact, it seems possible to arrive at the appropriate form of the SCZ thermal wind equation for this latter case via multiple routes; the advantages of theoretical models that lead to the coincidence of constant  $\sigma'$  and  $\Omega$  surfaces have been discussed elsewhere (Balbus 2009, BBLW, Schaan & Balbus 2011). In any case, such behavior enjoys very clear numerical support (Miesch et al. 2006).

The explicit bulk-SCZ and tachocline solutions, equations (21) and (25) respectively, work reasonably well even in the constant  $\beta$  limit, and strikingly well when  $\beta$  is permitted to vary. Only the details of the mathematical solutions, not their essential structure, are sensitive to the choice of free parameters. At this point there seems little doubt that thermal wind balance is, in fact, the overall organizing principle for the tachocline and interior SCZ.

We are, however, far from a complete solution. The mathematical equations contain free parameters, which must be chosen to fit the helioseismology data. We lack an understanding of how they are determined from first principles. For example, the existence of a tachocline “bifurcation point,” where the isorotation contours diverge either toward the pole or equator, is clearly a consequence of the  $\theta$ -independent boundary condition imposed by the uniformly rotating core. The location of this bifurcation point depends upon our  $\epsilon$  parameter, which reproduces the data well if  $\epsilon = 0.75$ , and much less well if  $\epsilon$  changes even by a little. Why  $\epsilon$  should be close to, but distinct from, the value of 0.8 (corresponding to vanishing viscous torque on the core) is not yet clear. Finally, the outer layers are not well understood.

Once again, the mathematical description of the isorotation contours seems simpler than the underlying physics that gives rise to them. A good match to the helioseismology data is obtained from an approach that uses thermal wind balance plus a simple  $\sin^2 \theta / (r - r_\odot)$  external source.

We may thus end on a positive note. If the work presented here is correct in its essentials, then the beginnings of a deeper dynamical understanding of the rotation of the solar convective zone are at hand. It is gratifying that there is a certain mathematical inevitability of the gross features of the Sun’s internal rotation pattern following from thermal wind balance and a tight coupling between the rotation and the residual entropy isosurfaces. It is likewise encouraging that the more complex appearance of the isorotation contours in the tachocline and outer layers seems to emerge from relatively simple mathematics. In short, there is no reason to think that the dynamics of the solar rotation problem is intractable. The blend of numerical simulation and analysis promises to be a powerful combination for elucidating the rotation profile of the convective regions of the Sun and of other types of stars.

### Acknowledgements

SAB is grateful to Princeton University Observatory for hospitality and support as a Paczynskii Visitor, and to the Isaac Newton Institute for Mathematical Sciences at Cambridge University, where this work was begun. We thank M. McIntyre and G. Vasil for their constructive comments on an earlier version of this work, and the referee for a helpful, detailed report.

### REFERENCES

- Balbus, S. A., 2009, MNRAS, 395, 2056
- Balbus, S. A., Bonart, J., Latter, H. N., & Weiss, N. 2009, MNRAS, 400, 176 (BBLW)
- Balbus, S. A., & Latter, H. N. 2010, MNRAS, 407, 2565 (BL)
- Balbus, S. A., & Weiss, N. O. 2010, MNRAS, 404, 1263
- Miesch, M. S., Brun, A. S., & Toomre, J. 2006, ApJ, 641, 618
- Miesch, M. S., & Hindman, B., 2011, arXiv:1106.4107v

Miesch, M. S., & Toomre, J. 2009, *Ann. Rev. Fluid Mech.*, 41, 317

Schaan, E., & Balbus, S. A. 2011, in preparation

Thompson, M. J., Christensen-Dalsgaard, J., Miesch, M. S., & Toomre, J. 2003, *ARAA*, 41, 599

### Appendix: the outer layers

The rotation pattern of the outer layers is characterized by a robust  $\sin^2 \theta$  angular pattern, and the stress associated with this seems to depend on radius as  $1/(r - R_\odot)$ . We assume that there are large scale poloidal velocity components in the outer layers, arising perhaps from turbulent stresses present in this region (Miesch & Hindman 2011). The introduction of nonuniform poloidal velocities  $v_r$  and  $v_\theta$  into the flow causes the  $\phi$  component of the vorticity,  $\omega_\phi$ , to come into existence. Because of our assumption of axisymmetry ( $\partial/\partial\phi = 0$ ) there are no changes at all to the poloidal components of  $\boldsymbol{\omega}$ . The addition of  $v_r$  and  $v_\theta$  velocities also do not cause any cross terms between  $\Omega$  and the poloidal components in the azimuthal vorticity equation. This means that the poloidal components of the velocity, which advect changes in  $\omega_\phi$ , behave as “external forcing” with regard to the angular velocity  $\Omega$  in the governing partial differential equation.

Start with the simplest possible circulation pattern consistent with quadrupolar symmetry,

$$v_\theta = A(r) \sin \theta \cos \theta. \quad (31)$$

Since mass conservation implies  $\nabla \cdot (\rho \mathbf{v}) = 0$ , the angular dependence of  $v_r$  must be the same as

$$\frac{1}{r \sin \theta} \frac{\partial(\sin \theta v_\theta)}{\partial \theta} = \frac{A}{r} (2 \cos^2 \theta - \sin^2 \theta) = \frac{A}{r} (3 \cos^2 \theta - 1) \quad (32)$$

In other words,  $v_r$  has the angular dependence of  $P_2(\cos \theta)$ . Letting

$$v_r = B(r) (3 \cos^2 \theta - 1) \quad (33)$$

we find that  $B$  and  $A$  are related to one another by the mass conservation equation

$$\frac{1}{\rho} \frac{d(\rho r^2 B)}{dr} = -rA \quad (34)$$

Next, we evaluate the terms in  $\rho \mathbf{v} \cdot \nabla (\omega_\phi / \rho r \sin \theta)$  from the vorticity equation (5). The terms involving the operator  $v_r \partial / \partial r$  are

$$\rho v_r \frac{\partial}{\partial r} \left[ \frac{1}{\rho r^2 \sin \theta} \frac{\partial(r v_\theta)}{\partial r} - \frac{1}{\rho r^2 \sin \theta} \frac{\partial v_r}{\partial \theta} \right] = \rho v_r \cos \theta \frac{d}{dr} \left[ \frac{1}{\rho r^2} \frac{d(rA)}{dr} + \frac{6B}{\rho r^2} \right], \quad (35)$$

which simplifies to

$$\rho B (3 \cos^2 \theta - 1) \cos \theta \frac{d}{dr} \left[ \frac{1}{\rho r^2} \frac{d(rA)}{dr} + \frac{6B}{\rho r^2} \right] \quad (36)$$

This leads to a forcing term that is directly proportional to  $P_2(\cos \theta)$ , which is not what is observed. By contrast, the terms involving  $v_\theta \partial / \partial \theta$  are

$$\frac{v_\theta}{r^3} \frac{\partial}{\partial \theta} \cos \theta \left[ \frac{d(rA)}{dr} + 6B \right] = -\frac{A \sin^2 \theta \cos \theta}{r^3} \left[ \frac{d(rA)}{dr} + 6B \right] \quad (37)$$

This gives a second forcing term proportional to  $\sin^2 \theta$ , which is consistent with the observations.

Gathering the two terms together,

$$\rho \mathbf{v} \cdot \nabla \left( \frac{\omega_\phi}{\rho r \sin \theta} \right) = \rho \cos \theta \left[ B (3 \cos^2 \theta - 1) \frac{d}{dr} - \frac{A \sin^2 \theta}{r} \right] \left[ \frac{1}{\rho r^2} \frac{d(rA)}{dr} + \frac{6B}{\rho r^2} \right] \quad (38)$$

which, on the right side, is equal to

$$\rho \cos \theta \left[ B (3 \cos^2 \theta - 1) \frac{d}{dr} + \sin^2 \theta \frac{1}{\rho r^2} \frac{d(\rho r^2 B)}{dr} \right] \left[ -\frac{1}{\rho r^2} \frac{d}{dr} \frac{1}{\rho} \frac{d}{dr} (\rho r^2 B) + \frac{6B}{\rho r^2} \right]. \quad (39)$$

Thus, there are two possible angular behaviors of the vorticity advection terms that emerge from the analysis:  $P_2(\cos \theta)$  and, possibly in superposition,  $\sin^2 \theta$ . For the outer layers, however, we require forcing that is proportional only to  $\sin^2 \theta$ . This means that the terms in the second square bracket of equation (39) must be a *constant*, which we denote as  $C$ . Standard models for the outermost layers in the Sun seem to give something close to  $\rho = \rho_0 (1 - x)^3$  for the density, where  $\rho_0$  is a characteristic density and  $x = r/R_\odot$ , the radius in units of the solar radius. Then, with  $u = 1 - x$ ,  $\rho = \rho_0 u^3$ , this constancy condition may be written as an inhomogeneous differential equation for  $B$ :

$$-\frac{d}{du} \frac{1}{u^3} \frac{d}{du} (u^3 B) + 6B = C R_\odot^2 \rho_0 u^3. \quad (40)$$

The solution for the homogeneous equation is

$$B \text{ (homo)} = c_1 \frac{I_2(u\sqrt{6})}{u} + c_2 \frac{K_2(u\sqrt{6})}{u} \quad (41)$$

and the inhomogeneous solution is (to leading order in small  $u$ )

$$B \text{ (inhomo)} = -\frac{u^5}{32}C\rho_0R_\odot^2 \quad (42)$$

The inhomogeneous solution is well behaved near the solar surface (i.e., for small  $u$ ), and the  $I_2$  solution is well-behaved at  $u = 0$ , but the  $K_2$  solution is singular. The mass flux, however, is finite. Moreover, the disturbance should disappear as we move into the convective zone, so that our solution must decrease with growing  $u$ . This is not compatible with  $I_2$ . We therefore retain the  $K_2$  solution—indeed, we are looking for singular velocity behavior near the surface. Then, for small  $u$  we have

$$A = -\frac{1}{\rho} \frac{d(\rho B)}{dx} = \frac{1}{u^3} \frac{d(u^3 B)}{du} \quad (43)$$

or,

$$A = \frac{c_1}{u^3} \frac{d(u^2 K_2(\sqrt{6}u))}{du} = \frac{c_1}{u^2 U} \frac{d(U^2 K_2(U))}{dU} \quad (44)$$

where  $U = \sqrt{6}u$ . Using a standard Bessel function identity, this becomes

$$A = -\frac{c_1}{u^2 U} U^2 K_1(U) = -\frac{c_1 U}{u^2} K_1(\sqrt{6}u) = -\frac{c_1 \sqrt{6}}{u} K_1(\sqrt{6}u) \quad (45)$$

Therefore, to extract a solution with  $\sin^2 \theta$  angular forcing in the outer layers from the assumed circulation pattern, the quantity  $\omega_\phi / (\rho r \sin \theta)$  and radial mass flux must both be constant with depth, and the  $\theta$  velocity sharply decreasing with depth.

If we now pull together the results of this mathematical excursion and return to equation (38) to determine the nature of the forcing we find i) it is rather straightforward to produce  $\sin^2 \theta$  forcing; and ii) the sign of the forcing can be chosen by a suitable choice of  $C$  and  $c_1$ . These are perhaps two important successes. But in spite of the singular behavior of the  $K_2$  function near the surface, in this model the vorticity stress is *not* singular. The regular behavior is due to the appearance of the surface density  $\rho$  in the equation, which vanishes at the surface. This is an important shortcoming of the model, as the data seem to require logarithmic “quasi-singular” behavior of the constant  $\Omega$  contours near the surface. It may be that this feature can be captured by a more careful consideration of the radially steepening entropy gradient, which has been neglected here, lying outside the scope of our analysis.

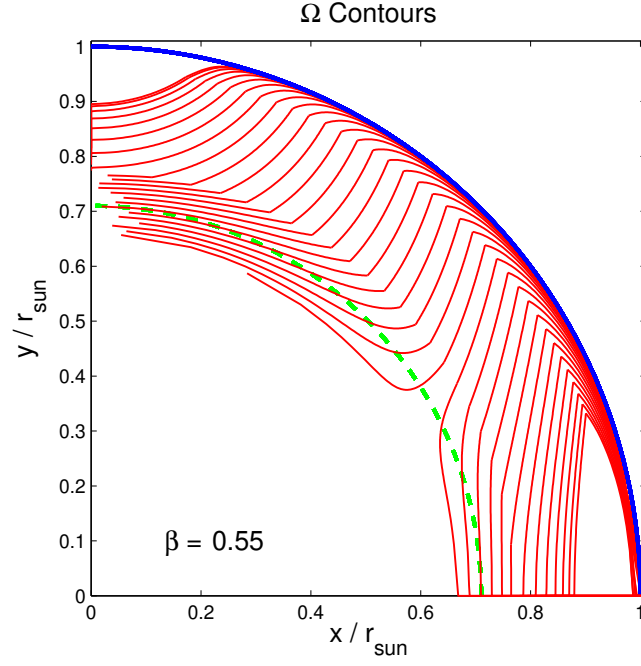


Fig. 1.— The isorotation contours of the Sun according to equation (25) with  $\beta = 0.55$ ,  $r_0 = 0.896$ ,  $r_1 = 0.96$ ,  $r_T = 0.77$  (solar radii),  $k_1 = 1.745$ .

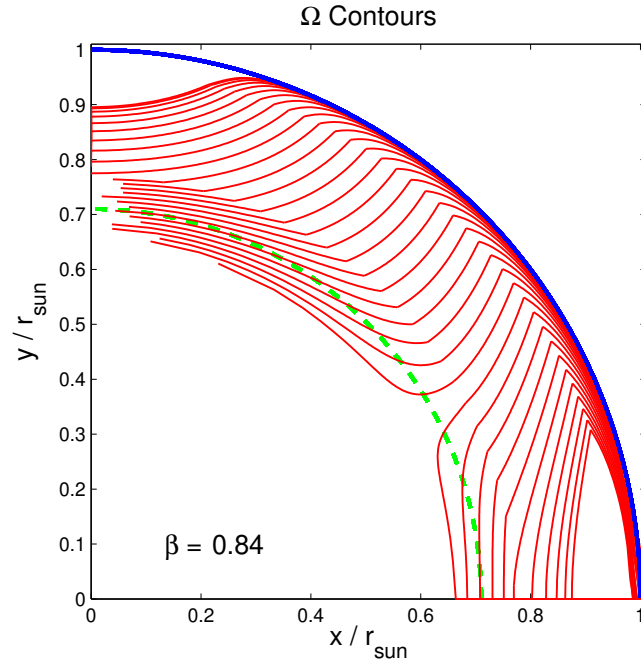


Fig. 2.— As in Fig. [1] with  $\beta = 0.84$ .

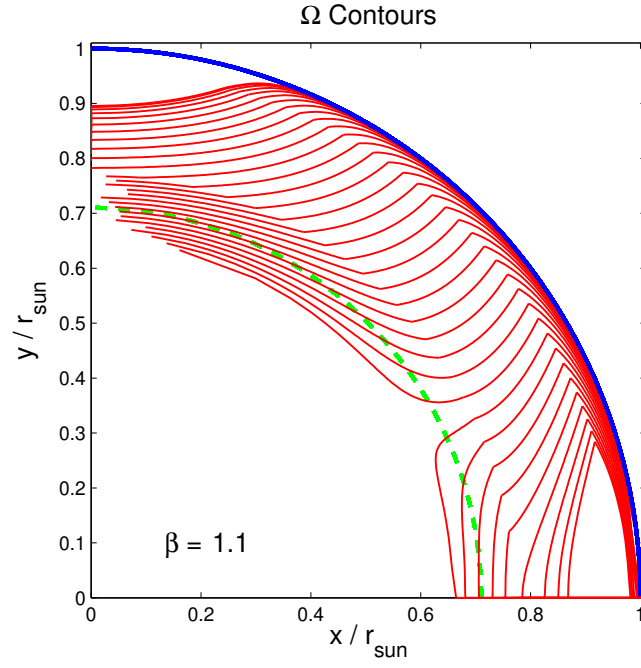


Fig. 3.— As in Fig. [1] with  $\beta = 1.1$ .

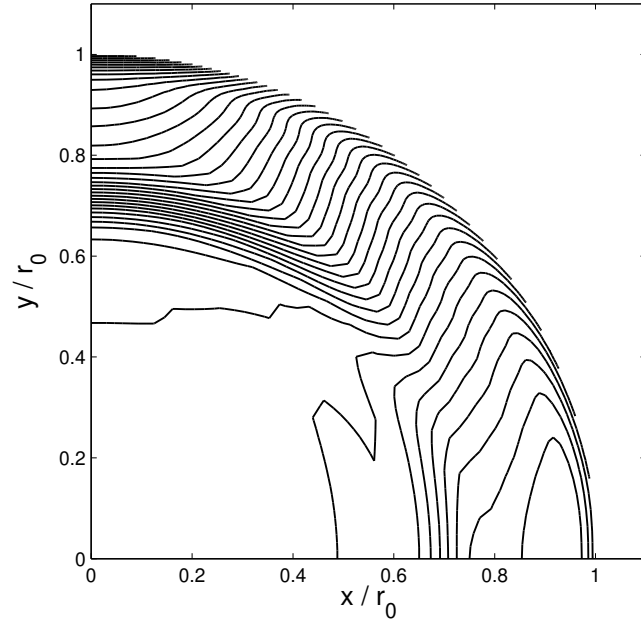


Fig. 4.— Global Oscillation Network Group (GONG) isorotation contours (courtesy R. Howe).

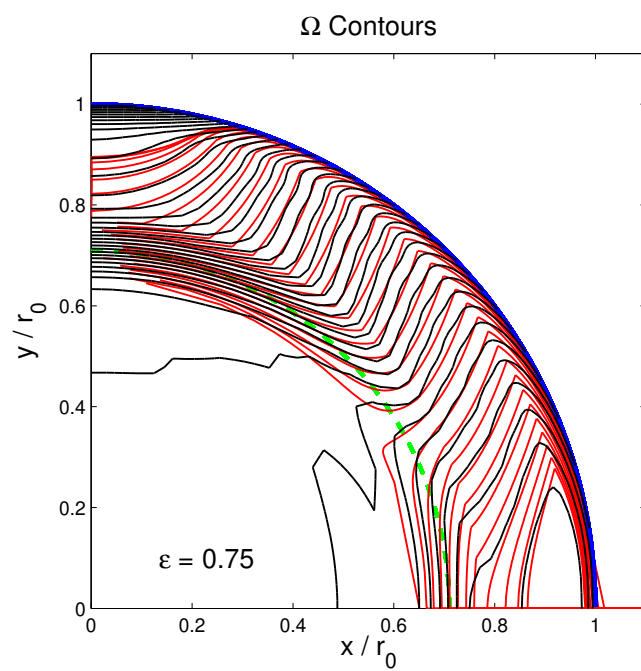


Fig. 5.— GONG data (black) overlayed with fit from equations (25) and (28) (red).  $\epsilon = 0.75$ . Other parameters as in Fig. [1]. The contours near the point of bifurcation at the radiative core are very well-modeled.



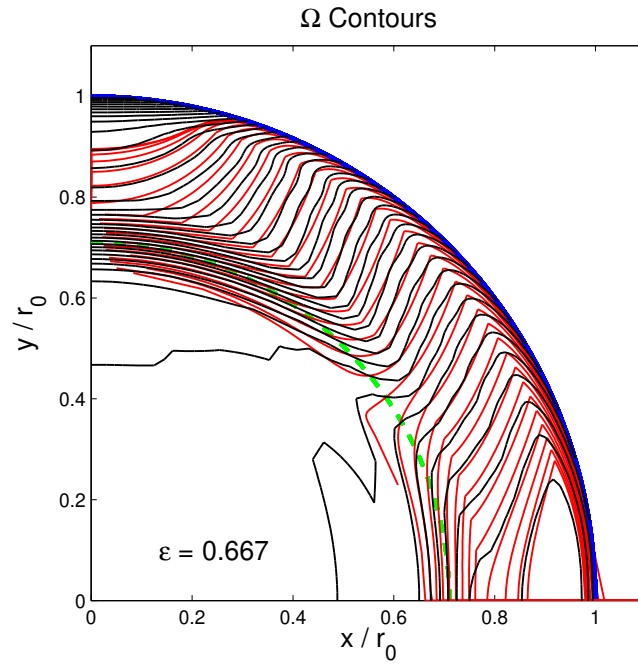


Fig. 6.— GONG data (black) overlayed with fit from equations (25) and (28) (red).  $\epsilon = 2/3$ . Other parameters as in Fig. [1].

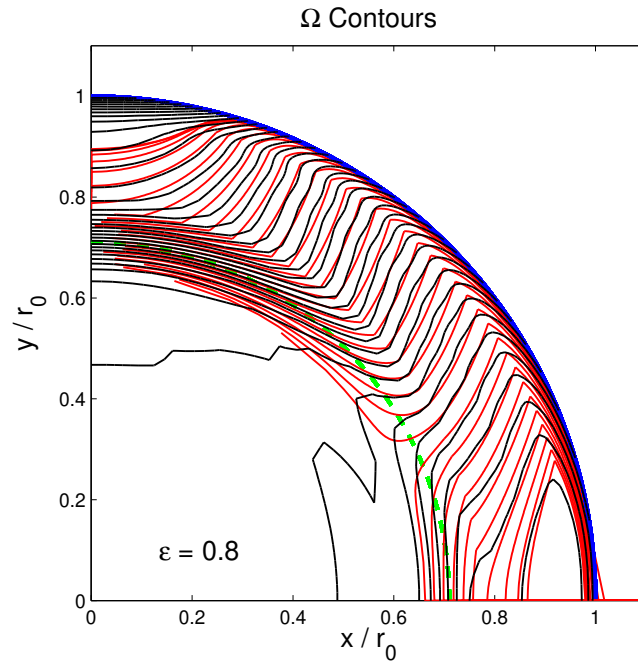


Fig. 7.— GONG data (black) overlayed with fit from equations (25) and (28) (red).  $\epsilon = 0.8$ . Other parameters as in Fig. [1].